

New Approach to System Server Air Flow/Thermal Design Development, Validation & Advancement in Green Fan Performance

Marlin Vogel, Tony Chen*, Steve Doan*, Howard Harrison**, Rajeech Nair***

Electronic Cooling Solutions and *Sun Microsystems
and **Distributed Thermal Systems and ***Degree Controls
email: mvogel@ecooling.com

Abstract

Increasing thermal demands of high-end servers require increased performance of air-cooling systems in order to meet industry requirements. Increased air cooling performance will be attained through efficient distribution of the air flow to multiple electronic modules and improved aerodynamic power conversion efficiency of the server air movers and incorporating inter-stage air flow directional control structure between tandem fans that are arranged in series air flow. A new approach is used to measure and validate air flow rates for the server's individual electronic modules. The new approach is intended to improve the accuracy of the air flow measurement and simplify the in-situ air flow measurement process, allowing reduced instrumentation cost and reduced time required to develop and validate the server air flow design.

Keywords

Air flow sensors, air movers, fans, aerodynamic power conversion efficiency, volumetric air flow rate

1. Introduction/Background

Next generation servers require efficient distribution of air flow to multiple electronic modules, while also minimizing the time required to develop, validate, and finalize the air flow and thermal design. For this study the system development effort consists of carrying out traditional detailed module level CFD flow analysis to predict the flow versus pressure loss characteristics; using an empirical approach to validate and finalize the predicted module level air flow characterization with unpowered module hardware mockup; carry out detailed system level CFD analysis using simplified flow characteristic modeling of the individual modules; calibrate hot wire velocity anemometers for simplified and detailed individual module mockups to characterize volumetric air flow rate versus in-

situ velocity measurements; and finally utilize the module air flow calibration characteristics to conduct in-situ measurement of individual module air flow rates along with measuring total system air flow rate.

Systems using multiple fans in a series air flow direction configuration typically experience a performance degradation for the downstream fan due to an adverse secondary swirl air flow direction being generated by the upstream fan's exhaust.

1.1 System Description

A side view of the system is illustrated in Figure 1.1. The overall outer dimensions of the system are approximately 74 in. (height) x 39 in. (depth) x 24 in. (width). The air inlet is located at the lower front region of the system. Approximately 10% ($M \sim 0.1$) of the total system air flow rate is routed through Modules B and exits through the lower aft region of the system. Approximately 90% of the air flow rate is distributed to Modules A and Modules C, located above the system air mover chassis, with approximately 60% ($M \sim 0.6$) of the total system air flow routed through Modules C, and approximately 30% ($M \sim 0.3$) is routed through Modules A. The air flow exits Modules A and Modules C, exhausting through the top of the system. Modules A dimensions are approximately 26 in. (height) x 12 in. (depth) x 2.1" (width) for each individual module. Modules B dimensions are approximately 26 in. (height) x 24" (depth) x 1.75" (width) for each individual module. The air plenum height between the fan chassis exit and the Modules A and Modules B air inlet is approximately 4 in. The air plenum height between Modules C and below the fan chassis is approximately 8 in.

The air mover chassis consisted of 12 sets of tandem fans. The outer dimensions of the individual fans was 172mm x 150mm x 50mm. The total depth of the fan chassis was 150mm, with the inlet of the upstream (primary) fan located was at the bottom of the fan chassis,

and the exit of the downstream (secondary) fan was located at the top of the fan chassis. A flow optimizer with a flow length of 50mm was located between each set of tandem fans in order to increase the performance of the secondary fan.

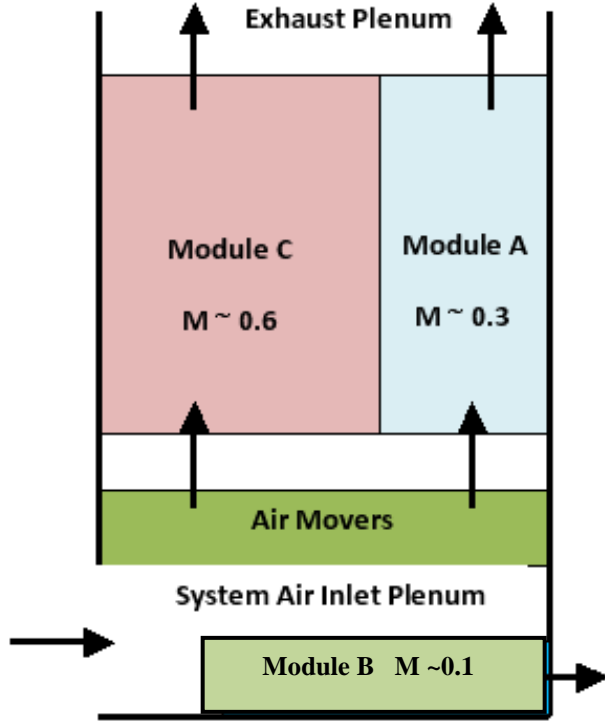


Figure 1: Illustration of system (side-view), not to scale.

2. Test Setup

2.1 Module A Mockup

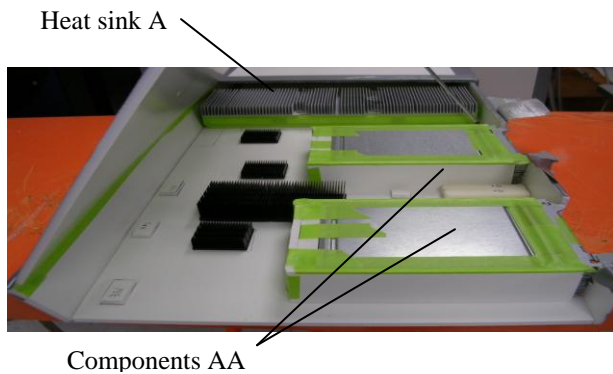


Figure 2: Module A mockup

An air flow mockup of Module A containing the primary components is shown Figure 1.2. The air inlet region of Module A contains heat sink A [1] that spans the full width of the module. All the air entering the module is ducted

through heat sink A, with the heat sink contributing the majority of the total module pressure loss. The air flow module was tested with three different heat sinks which had uniform fin densities of 8 fins per inch, 12 fins per inch and 15 fins per inch. All three heat sinks had a fin height of 18mm, and the fin thickness of 0.5 mm. Components AA are located in the downstream section of Module A. The air flow mockup was tested with components AA fully open and fully closed to represent the minimum and maximum pressure loss conditions. The fully closed components A are shown in Figure 2.

In order to expedite the system level air flow air flow characterization the flow mockup of Module A containing the individual components was replaced by a mockup that has the same outer dimensions of Module A, with a continuous, uniform, rectangular cross sectional area that extends throughout module, and yields the equivalent pressure loss characteristics exhibited by the module containing the individual components. The exit area of the simplified Module SA, is shown in Figure 3. The width of the opening was approximately 0.5", and was varied accordingly to yield required pressure loss characteristics.

In order to expedite the system level air flow characterization, the module SA mockup contained a single, commercially available hot wire anemometer [2] located approximately at the midpoint of the exit cross sectional area. The module was placed in a calibrated wind tunnel, and the sensed velocity from the hot wire anemometer was calibrated to indicate the module volumetric flow rate. If the acceptable linearity is attained, then the volumetric flow rate as measured by the single sensor would be considered to be a reasonably accurate measurement. Traditionally, in order to measure volumetric air flow rates, multiple hot wire anemometers are located within the cross sectional plane, and the volumetric flow rate is calculated as the product of the cross-sectional area for the air flow and the average flow velocity sensed by the hot wire anemometers. With final calibration performed by using an ASTM certified wind tunnel, with flow range and linearity verified. In order to attain added confidence in using a single sensor for each module SA, calibration testing was conducted with a group of 3 modules, a group of 5 modules, and finally a group of 8 modules, shown in Figure 4, representing the aft region of the server sub-system. The module pressure loss at the estimated system level and resulting module SA flow rates yields relatively high back pressure flow conditions, potentially allowing the simplified module SA internal duct design to exhibit consistent flow straightening characteristics, and thereby enabling valid volumetric flow rate measurements to be attained at the module exit when the system fans deliver air flow with secondary swirl directional components to the module inlet.



Figure 3: Module SA (simple) mockup



Figure 4: Calibration setup for sub-system level mockup of modules SA

2.2 Module C Mockup

A final version of the Module C mockup was available from a previous development program. The module flow characteristics, pressure loss as a function of volumetric flow rate, were measured through the use of a calibrated wind tunnel. Similar to the above module SA mockup simplification, two hot wire anemometers [2] were located approximately at equally spaced locations at the exit cross sectional area for each of the Module C mockups. The modules were placed in a calibrated wind tunnel, and the sensed velocity from the hot wire anemometer was calibrated to indicate the module volumetric flow rate. Again, if acceptable linearity is attained, then the volumetric flow rate as measured by the two sensors per module would be considered to be a reasonably accurate measurement. Similar to Module A and the simplified Module SA, the Module C back pressure and orientation of the internal components provide good potential to straighten swirl component of the air flow direction being delivered by the fans into the inlet of the Modules C in the system mockup.

2.3 Preliminary Sub-System Mockup - Modules A

The sub-system containing Modules A was simulated through using a group of 8 SA modules in conjunction with

6 tandem fan sets. The actual system fan chassis is designed to have an the one-half the diameter of an additional 3 tandem sets of fans deliver air to the Modules A. The preliminary sub-system test set up is shown in Figure 5. Test matrix included measuring the total sub-system air flow rate while also measuring the individual module air flow rates for conditions when all the fans are operational, conditions of single fan failure, and conditions for single fan tray failure. The sub-system air flow characterization included testing with a 50mm and a 100mm inlet plenum flow length between the sub-system fan tray mockup and the SA modules inlet.



Figure 5: Test setup for preliminary Modules A sub-system.

2.4 Full System Mockup

The full system mockup utilized the simplified Modules SA and the mockup Modules C. Similar to 2.3, the full system air flow test matrix included having all of the fans operational, single fan failure, and single fan tray failure for the region of the fan chassis that yielded the minimum air flow rate for the Modules A sub-system, along with the Modules C sub-system. Additionally, the plenum depth between the Modules B and the inlet of the fan chassis was varied in order to determine the optimum system inlet plenum depth.

2.5 Tandem Fan Performance Validation

Fans were selected from 4 different suppliers. Single tandem fan set aerodynamic performance was validated for each of the supplied fan designs with and without the use of an inter-stage structure, flow optimizer, which potentially corrected the swirl component of the air flow direction exiting the primary fan, prior to the air flow entering the secondary fan.

The added performance provided by a flow optimizer used with 120mm diameter tube axial tandem fans, aligned in a series air flow path successfully demonstrated [3] , [4] addressing potential issues of swirl between the primary and secondary fans. The multistage flow optimizer was designed to (i) convert swirl kinetic energy into axial kinetic energy and (ii) reduce swirl down to a residual level at inlet to secondary fan. The measured results for the 120mm dia. fans demonstrated performance levels that exceeded the theoretical two fan maximum, based on manufacturer's specification; and showed that the same flow optimizer design was applicable to all fan

manufacturers considered. The goal for this development effort is to attain performance enhancements for the 172mm diameter tube axial fan tandem fan sets that are comparable to the performance enhancements previously attained with the 120mm diameter tandem fans.

The flow optimizer supplier carried out design and verification testing at their facility. The test set-up included a standard flow bench, based on ANSI/AMCA 210-99, 172 mm x 150 mm fans from four different suppliers, and DTS flow optimizers. The single fan and two fan configurations were connected directly to the flow bench inlet baffle, through a cut-out that complied with the fan manufacturer’s recommended outlet geometry. Four fan configurations were also connected to the flow bench through an ANSI standard inlet reducer, to accommodate the wider geometry of two parallel sets of series fans. Each test was repeated until at least two sets of test results were in reasonable agreement. Then, the results were averaged and corrected to standard conditions using the ANSI recommended methodology.

Each single fan was first tested to ensure that it complied with the manufacturer’s specification, and then labeled for reference purposes. These single fan tests were repeated periodically throughout the process to confirm repeatability, both for the fans and the flow bench itself.

The series tests were configured with two fans separated by a sealed gap of 50 mm. Hence these tests were completed to establish the baseline series performance for each of the three fan suppliers. These were followed by the optimized tests, which were configured with a DTS flow optimizer in the 50mm gap between the fans, to determine the increased performance and therefore the thermal headroom that could be achieved with the optimized configuration. It is important to note that the *same* flow optimizer was used with fans from all three fan suppliers, even though some fans had exit stators while others did not.

Next, the series tests were repeated with two parallel pairs of series fans, to duplicate the existing configuration and establish the baseline performance. Flow optimizers were then installed between the of fans to compare actual vs. calculated performance, based on the results of the two fan optimized tests and the parallel fan law, in order to confirm that there were no unexpected losses at the parallel inlets. It is important to note that the optimized pairs remained independent, i.e. each pair of fans was connected through an independent flow optimizer and the airflows were not allowed to mix. The initial tests at 100% PWM were followed by subsequent tests at reduced PWM until the operating point objective of 520 CFM @ 1.8” H₂O was achieved. Current readings at that point were used to determine the reduced power required by, and therefore the power savings that could be achieved with, the more efficient four fan optimized configurations.

Final performance validation test work was conducted at Sun Microsystems. In addition to the flow optimizer development, the tandem fan set aerodynamic performance was characterized for 3 different finger guard designs,

which were located at the inlet of the primary fan, and the exit of the secondary fan.

3 Test Results & Discussion

3.1 Module A, SA, and C mockups

| Config | Comp. “AA” dP model | Heat sink A - fins per inch | Module A Pressure loss (in. H ₂ O) | Module SA Pressure Loss (in. H ₂ O) |
|--------|---------------------|-----------------------------|---|--|
| A.1 | minimum | 8 | 0.51 | na |
| A.2 | “ | 12 | 0.72 | na |
| A.3 | “ | 15 | 0.97 | na |
| A.4 | maximum | 8 | 0.62 | 0.67 (1) 0.67 (3) |
| A.5 | “ | 12 | 0.78 | 0.82 |
| A.6 | “ | 15 | 1.14 | na |
| C | na | na | 0.75 | na |

Table 1: Measured Module A (100 cfm), Module SA (100 cfm) and Module C (250 cfm) pressure loss

The measured pressure loss for the Modules A, SA and C are shown in Table 1. The anticipated flow requirements for Module A is 80 to 100 cfm, and 200 to 250 cfm for Module C. The measured results show that increasing the Heat sink A fin density from 8 fins per inch to 15 fins per inch yielded a 90% increase in the module pressure loss for Configurations A.1 to A.3, and a 84% increase in the module pressure loss for Configurations A.4 to A.6. A increase of ~20% in the Module A pressure loss occurred when comparing Components AA being fully open versus being fully closed. Config A.2 and A.5 Results in Table 1 also show that the simplified module mockup, SA, provided comparable module pressure losses for Configurations A.4 and A.5. At the projected maximum module air flow requirements and heat sink A fin density, Module A (Configuration A.5) and Module C yielded comparable pressure losses.

3.2 Sub-System SA & System Mockups

The SA modules that yielded the higher pressure loss shown in Table 1 were utilized for the Sub-System and full system mockup flow characterization test work. The results shown in Table 2 indicated that for the sub-system with the SA modules, only, increasing the inlet plenum depth between the fan chassis and the SA modules from 2” to 4” yielded a 3% increase in the average Module SA flow rate when all fans were operational. The sub-system results also indicated that 4” plenum yielded a 7% increase in the

minimum module air flow rate for single fan failure as compared to the 2” plenum results.

| Config. | Inlet Depth | Fan Fail | Average Module Flow rate (cfm) | Minimum Module Flowrate (cfm) |
|-------------|-------------|----------|--------------------------------|-------------------------------|
| Sub-Syst SA | 2” | no | 100 | na |
| “ | “ | yes | 93 | 83 |
| “ | 4” | no | 103 | na |
| “ | “ | yes | 95 | 89 |
| System | 4” | no | SA: 120 C: 191 | SA: 113 C: 180 |

Table 2: Measured module air flow rates for the sub-system SA (A) modules and the system mockup.

The full system mockup results show that SA modules average and minimum module flow rate exceeded the projected requirement (80 to 100 cfm) with margin. The full system mockup results also indicated that the average and minimum measured flow rates for Modules C were 5% to 10% below the minimum requirement (200 cfm). The preliminary system results indicated that total fan were meeting the total minimum system flow requirements (2000 cfm), but design provisions may be required to provide additional flow balancing in order to re-distribute air flow from the Modules A to the Modules C.

3.3 Production System Prototype

Tables 3 and 4 contain the volumetric air flow sensor calibration data for the production level Modules A and Modules C. The calibration data shows that acceptable linearity relationship was attained for all of the modules between the sensed velocity and the calibrated volumetric air flow rate.

| Module # | 75 cfm | 100 cfm | 125 cfm | 150 cfm |
|----------|--------|---------|---------|---------|
| 1 | 758 | 1006 | 1265 | 1558 |
| 2 | 706 | 925 | 1115 | 1354 |
| 3 | 786 | 1048 | 1291 | 1588 |
| 4 | 770 | 1021 | 1267 | 1538 |
| 5 | 763 | 1002 | 1224 | 1478 |
| 6 | 753 | 1001 | 1225 | 1491 |
| 7 | 642 | 879 | 1135 | 1393 |
| 8 | 817 | 1056 | 1293 | 1563 |

Table 3: Module A volumetric flow sensor calibration data

| Module # | 150 cfm | 200 cfm | 250cfm |
|----------|---------|---------|--------|
| 1a | 1122 | 1457 | 1839 |
| 1b | 1042 | 1355 | 1695 |
| 2a | 1194 | 1497 | 1866 |
| 2b | 1055 | 1380 | 1763 |
| 3a | 1095 | 1415 | 1787 |
| 3b | 1091 | 1413 | 1754 |
| 4a | 1243 | 1664 | 2089 |
| 4b | 1086 | 1434 | 1828 |
| 5a | 1080 | 1386 | 1751 |
| 5b | 1190 | 1573 | 1995 |
| 6a | 1205 | 1542 | 1909 |
| 6b | 1138 | 1517 | 1971 |
| 7a | 1116 | 1452 | 1845 |
| 7b | 1098 | 1446 | 1841 |
| 8a | 1069 | 1376 | 1735 |
| 8b | 1112 | 1443 | 1824 |

Table 4: Module C volumetric flow sensor calibration data

| Single Fan Fail | Fan Duty Cycle | Wind Tunnel (cfm) | Summation of Module (cfm) | Minimum Module Flowrate (cfm) |
|-----------------|----------------|-------------------|---------------------------|-------------------------------|
| No | 100% | 2860 | 2759 | A: 122 C: 211 |
| No | 80% | 2645 | 2432 | A: 108 C: 187 |
| Yes | 100% | 2726 | 2593 | A: 119 C: 195 |

Table 5: Measured total system and minimum module air flow rates.

The results shown in Tables 5 shows that there is relatively good agreement between the total measured air flow when using a calibrated wind tunnel versus summation of the individual module air flow rates as measured with the calibrated follow sensors. The results shown in Table 5 also indicates that the total minimum system air flow requirements (2000 cfm) are attained with margin for all conditions, and the minimum module air flow requirements are attained at the 100% duty cycle with all fans operational. The results also indicate that with a single fan failure, the minimum required air flow rate is attained for all modules A, and the minimum flow rate Module C is only 2.5% below the requirement (200cfm). The results also show that there is good potential to reduce the duty

cycle at lower ambient air temperature conditions and still meet the thermal module thermal requirements, thereby reducing data room energy costs

3.4 Fan & Tandem Fan Configurations

It can be seen from Figures 6, 7, 8, and 9 that the optimized performance exceeded the series performance for all four manufacturers, at all flow rates. Further, Table 6 shows that the aero output power increased from 13.7% to 46.7%, or an average of 24.2%, expressed as a percentage of the existing or series performance. This is significant given that the flow optimizer is simply a passive device that is installed between the fans. It is also important to note that these increases are net of any drag effects of the flow optimizer, i.e. the actual increase is actually greater than reported because these numbers have already been reduced by the incremental drag introduced by the flow optimizer's internal components.

Figures 10, 11, 12, and 13 illustrates the increase in aero efficiency, expressed as aero output power relative to electrical input power. Again, it can be seen that the optimized configuration operates at a higher efficiency across the entire operating range, with greater gains realized at the higher flow rates. It is also important to note that the aero efficiency of the optimized configuration actually exceeded that of the underlying single fans, likely due to the fact that the secondary fan is operating at above the manufacturer's specification, due to the energy recovered by the flow optimizer from the output of the primary fan.

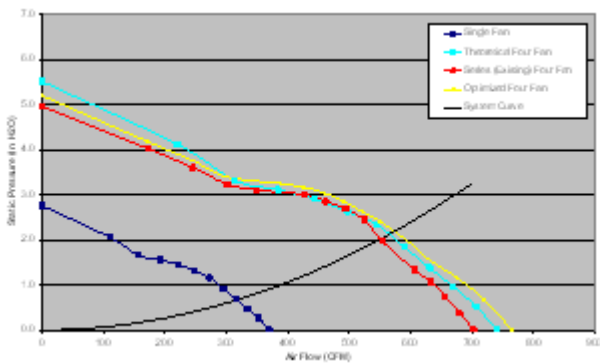


Figure 6: Measured performance of Supplier A fans

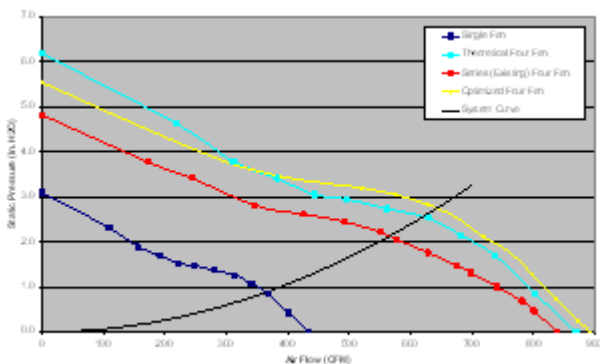


Figure 7: Measured performance of Supplier B fans

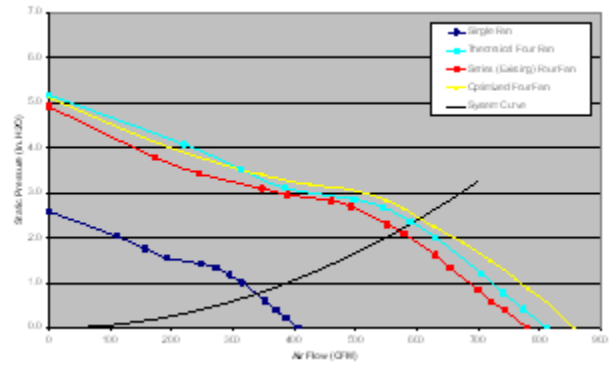


Figure 8: Measured performance of Supplier C fans

Increased efficiency allowed the PWM input to be reduced while still achieving the desired operating point (520CFM @ 1.8" H₂O), as seen in Figure 14. Table 7 shows the an average power savings of 72 watts or 21.1%, relative to the initial power budget of 340 watts for the desired operating point. It is not surprising that Supplier B produced the greatest power savings since the fans from this supplier also provided the greatest increase in aero output power (46.7%) when the flow optimizer was installed.

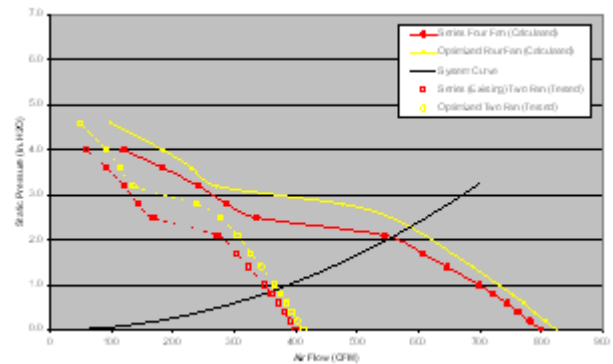


Figure 9: Measured performance of Supplier B fans

| Fan Supplier | Optimized Performance (CFM @ In H ₂ O) | Existing Performance (CFM @ In H ₂ O) | Increase of Existing Performance |
|--------------|---|--|----------------------------------|
| A | 574 @ 2.19" | 550 @ 2.01" | 13.7% |
| B | 643 @ 2.75" | 566 @ 2.13" | 46.7% |
| C | 605 @ 2.44" | 570 @ 2.16" | 19.9% |
| D | 586 @ 2.29" | 557 @ 2.07" | 16.4% |

Table 6: Increased fan operational performance

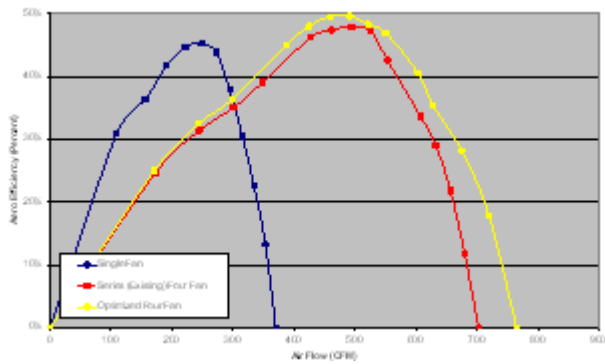


Figure 10: Fan efficiency performance for supplier A

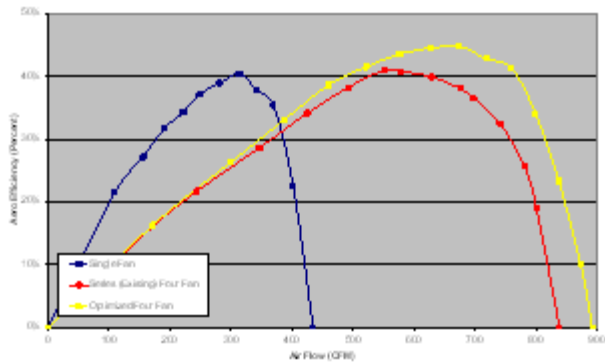


Figure 11: Fan efficiency performance for supplier B

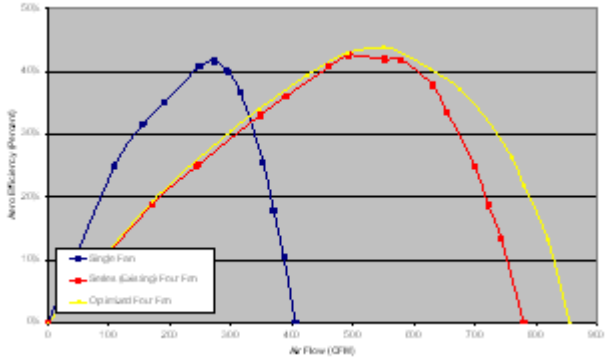


Figure 12: Fan efficiency performance for supplier C

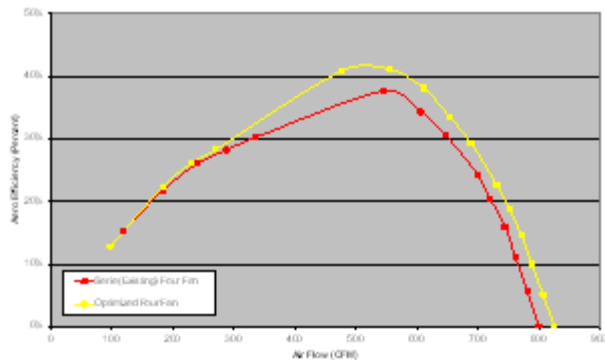


Figure 13: Fan efficiency performance for supplier D

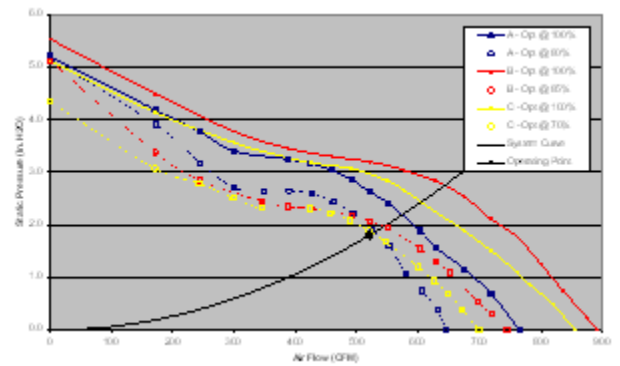


Figure 14: Reduced PWM operation of fans from suppliers A,B, &C, to achieve the projected operating point

| Fan Supplier | PWM Control Point | Reduced Power (Watts) | Percent Power Savings |
|--------------|-------------------|-----------------------|-----------------------|
| A | 79% | 267 | 21.4% |
| B | 81% | 255 | 25.0% |
| C | 68% | 283 | 16.8% |

Table 7: Optimized power savings at the projected operating point (allocated power is 340W per four fans)

4 Conclusions

Utilizing simplified module air flow mockups in combination with hot wire anemometers calibrated to sense the module volumetric flow rates enabled the preliminary thermal design feasibility effort to be expedited through an empirical approach. The air flow design feasibility validated 9 months prior to attaining the first production level system. Calibrating the hot wire anemometers to directly sense the volumetric flow rate for the production level modules allowed the final air flow performance validation to be expedited while yielding accurate in-situ air flow measurements of the individual modules for the production level prototype system.

It was found that locating the flow optimizer in between the upstream and downstream fans modified the air flow pattern for the downstream fan inlet, allowing the aerodynamic output performance for 4 candidate fan suppliers to be increased by an average of greater than 20% for constant fan input power, with very little impact on fault mode performance. Or, the flow optimizer allowed the required aerodynamic performance to be attained with an average reduction of at least 20% in fan input power for all candidate fan suppliers. In the latter case the fans operated at a reduced and more consistent rpm, reducing acoustic noise and extending the expected life of the fans. This improved performance was attained for the full range in required air flow conditions as determined for maximum and minimum ambient supply air temperatures.

Depending on the supplied ambient air temperature, the required fan input power without the inter-stage flow structure can be as great as 15% of the total input power to the server. Assuming that the total server input power is 10 kW, incorporating the use of the inter-stage flow optimizer will provide an annual energy cost savings of approximately \$600 for data rooms utilizing traditional CRAC units, assuming a typical data room COP equal to 2.0, assuming 24/7 operation of the server, and assuming an electrical cost rate of \$0.15 per kW-hour. Although these results were achieved with 172mm fans, initial testing with 120 mm fans indicates that the enhanced performance and the associated benefits are scalable to other server formats.

References

1. M. Vogel, G. Xu, D. Copeland, S. Kang, B. Whitney, G. Meyer, K. Kawabata, and M. Connors, "Low Profile Heat Pipe Heat Sink & Green Performance Characterization for Nxt Generation CPU Module Thermal Design", 2009 IMAPS Advanced Technology Workshop on Thermal Management
2. Degrees Control, Accusense line of thermal anemometers, UAS1000 series - USB based airflow sensors.
3. J.Jilesen, H. Harrison, F. Lien, D. McCumber. "Multiple High Performance Dual Redundant or DR FanTM Modules Optimized For 1U Server Processor Upgrade Program", IThERM 2006.
4. J. Jilesen, et al. "Investigation of increased performance of close series stacked tube axial fans due to inclusion of diffuser element", Microelectronic Reliability (accepted in 2005, inpress).